Oceanic methane layers: the hydrocarbon seep bubble deposition hypothesis

I. Leifer[1]* and A. G. Judd[2]

[1]*Chemical Engineering Department, University of California, Santa Barbara, USA;* [2]*Applied Geology, University of Sunderland, UK*

ABSTRACT

Bubble plumes from hydrocarbon seeps drive upwelling flows in the water column that can disappear if the bubbles dissolve. This may lead to formation of a layer enriched in gases and substances transported by the bubbles, a process we term bubble deposition. A review of observed dissolved methane layers in the North Sea showed their existence in an area of active seeping pockmarks at a height of ~ 20–30 m above the sea bed, well below the thermocline. To test the bubble deposition hypothesis, rising seep bubbles were simulated numerically. The model predicted a dissolution depth consistent with the observed methane layer for ~ 2700-μm-radius bubbles. The model also predicted that bubbles smaller than 3400 μm dissolved subsurface, decreasing to 2000 μm for a 10-cm s^{-1} upwelling flow. We speculate that this layer may be attractive to marine organisms. Although North Sea seeps are not oily, this mechanism also applies to oily bubbles from hydrocarbon seeps or a leaking undersea gas/oil pipeline. Thus bubble deposition can create a subsurface oil layer which rises far slower than either the bubble stream or droplets entrained in the stream.

Terra Nova, 14, 417–424, 2002

Introduction

Natural marine hydrocarbon seeps are widespread features (Fleischer *et al.*, 2001) which potentially have an important impact on the cycling of hydrocarbons between the lithosphere, the hydrosphere, and the atmosphere (Hornafius *et al.*, 1999; Judd, 2000; Kvenvolden *et al.*, 2001; Judd *et al.*, 2002). They create a unique bio-geochemical and fluid-dynamical environment (Leifer *et al.*, 2000) not easily reproducible in the laboratory, and may have significant impact on the coastal and the global environment (Kvenvolden *et al.*, 2001), as well as 'simulating' many of the processes in an underwater oil/gas spill – see Johansen (2000) for a description of underwater spill processes.

Unlike deep-water seeps, the impact of seeps on the ecology in shallow continental shelf waters remains unclear. Some authors who worked on seeps in the North Sea – e.g. Hovland and Thomsen (1989) – or the Oregon continental shelf – e.g. Juhl and Targon (1993) – suggest a significant increase in biological activity around seeps. Others who worked on North Sea seeps – e.g. Dando *et al.* (1991), Dando and Hovland (1992) and Dando (2001) – argued that anomalous biological activity was accounted for mainly by the presence of hard ground (rocks of methane-derived authigenic carbonate) and a relatively sheltered environment. However, the presence of certain species with endosymbiotic chemosynthetic bacteria indicates some impact on benthic communities. These seep biology investigations were concerned primarily with benthic ecology. Despite speculation regarding the wider biological impact of seeps (Judd and Hovland, 1989), concerted efforts to study the biological seep implications higher in the water column are lacking.

Many of the unique seep conditions result from the presence of rising bubbles. At natural seeps, free gas bubbles rise from the seabed into the water column. Some seeps are little more than gentle emanations of bubbles from a few vents, while others bubble vigorously from dense vent clusters. Bubbles exchange gas with the surrounding fluid (Keeling, 1993), introduce turbulence (Monahan and Spillane, 1984), induce bulk fluid motions (Chen *et al.*, 1994), and efficiently transport oil and particles (Blanchard, 1989). However, the mechanisms for many of these processes are at best poorly understood – see Jakobsen *et al.* (1997) for a review. In some ways, a rising bubble plume is similar to a submerged buoyant jet, such as sewage or power plant discharges that rise in a stratified fluid until a terminal height (Zheng and Yapa, 1998), but important differences can arise. In a buoyant jet, all plume fluid elements contribute to buoyancy. Thus to model a seep as a buoyant jet, the buoyancy arises from decreased plume density due to the bubbles. But in reality, the fluid motion in a bubble plume is primarily due to discrete, highly buoyant elements, the bubbles, transferring momentum to the plume fluid. As a result, interesting properties may occur when the bubbles dissolve and the driving buoyancy force ceases. In this paper, we review observations of methane layers below the thermocline and discuss the implications of bubble dissolution on hydrocarbon seep bubble plumes and present observations best explained by a process we term bubble deposition.

Observations

The observations upon which this study is based were made at three locations: the UK sector of the North Sea (Summer 1991); the Santa Barbara Channel, California (Spring & Summer 2001); and the Gulf of Mexico (Summer 2000).

North Sea

Active pockmarks in UK Block 15/25, North Sea (shown in Fig. 1), have been subjected to numerous investigations (Hovland and Sommerville,

*Correspondence: Dr Ira Leifer, Chemical Engineering Department, University of California, Santa Barbara, CA 93106–5080, USA. Tel.: 805 8934941; fax: 805 8934731; e-mail: ira.leifer@bubbleology.com

© 2002 Blackwell Science Ltd

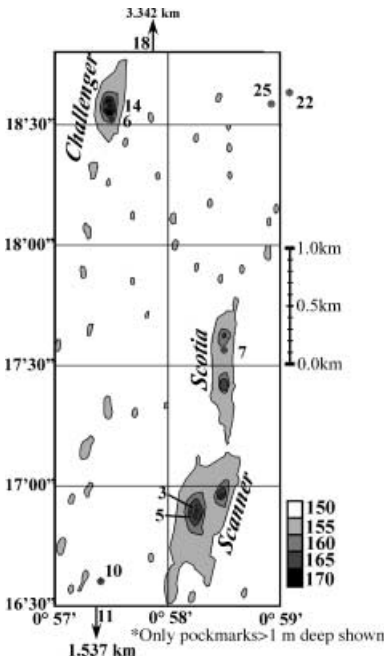

Fig. 1 Map showing pockmarks *Scanner*, *Scotia* and *Challenger* in the North Sea, UK Block 15/25. All were actively seeping gas. Data from multibeam echo sounder survey, *Kommander Jack*, April 2001 (courtesy of Geotek Ltd). Sample measurement sites shown. Arrows indicate sites off the map with distance to site from arrow base. Depth contour key and distance scale on figure. Grid lines show latitude (North) and Longitude (East).

1985; Hovland and Judd, 1988; Dando *et al.*, 1991; Judd *et al.*, 1994). ROV and manned submersible dives have confirmed that acoustic plumes show seepage activity. However, both the density of active vents and bubble flux are low (Hovland and Judd, 1988). High-resolution seismic profiles across this pockmark (Fig. 2) show hyperbolic water column targets. These were all at approximately the same height above the seabed (~ 20–30 m) but with a different character from the plumes associated with bubble.

Gulf of Mexico

Natural oil and gas seepage in the Gulf of Mexico is well documented (Brooks *et al.*, 1984; MacDonald *et al.*, 1999) and produces bubble plumes that have been observed by their acoustic return signal rising hundreds of metres. These signals often disappear before reaching the surface – e.g. Fig. 3. Previous authors noting this phenomenon (e.g. Guinasso and Schink, 1973; Judd *et al.*, 1997) have attributed it to one or more of the following: the gas bubbles passing out of the acoustic beam, the relationship between bubble size and acoustic signal being no longer conducive to acoustic resonance reflection, or dissolution of the gas bubbles. The transect in Fig. 3 was in the downcurrent direction, and thus the likely explanations are bubble dissolution or bubble dispersion at the same depth as the upper scattering layer. The upper scattering layer was most likely due to zooplankton, since it became thinner and shallower at night time. A second scattering layer was observed 60–80 m above the seabed, and showed no diurnal variation.

Santa Barbara Channel

The northern margin of the Santa Barbara Channel contains some of the most active areas of hydrocarbon seepage in the world, releasing both oil and gas (Hornafius *et al.*, 1999; Quigley *et al.*, 1999). Gas bubbles, to which the oil adheres, boil out of densely clustered vents. These seeps are very shallow (20–70 m) and seep bubbles are observed easily at the surface (Leifer *et al.*, 2000).

Bubbles and fluid motions

Few published quantitative observations of the bubble emission size distribution for hydrocarbon seeps exist. Bubble probability distributions from the Gulf of Mexico (GOM) and Santa Barbara Channel (SBC) are shown in Fig. 4. The GOM distribution was at the seabed (540 m deep) and represented bubbles escaping in a single, steady stream (Leifer and MacDonald, unpublished results). A pulsing stream at the same site (not shown) had a broad and flat distribution to 10^4-μm radius, r, unlike the distribution shown in Fig. 4. The SBC distribution was at the surface (i.e. 20 m above the seabed) for Shane Seep (34°24.37′N, 119°53.41′W) and represented bubbles rising from numerous vents, both pulsing and steady, located within a few metres of two adjacent and active pockmarks on the seabed. Both distributions decreased steeply from peaks at $\sim r = 2700$ μm.

Quantitative bubble distributions were unavailable for the North Sea, but visual observations suggested that some vents emitted continuous streams of ~ 2500-μm-radius bubbles, and in a narrow size range. Other vents intermittently released bursts of

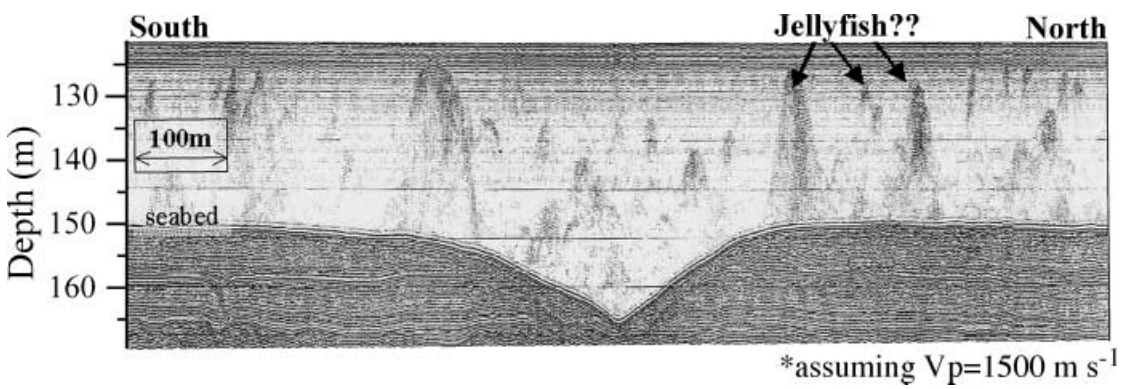

Fig. 2 Seismic profile of the '*Scanner*' pockmark, UK Block 15/25, North Sea (see Fig. 1 for locations). British Geological Survey (BGS) digital deep-towed boomer, previously published in Judd *et al.* (1994).

 © 2002 Blackwell Science Ltd

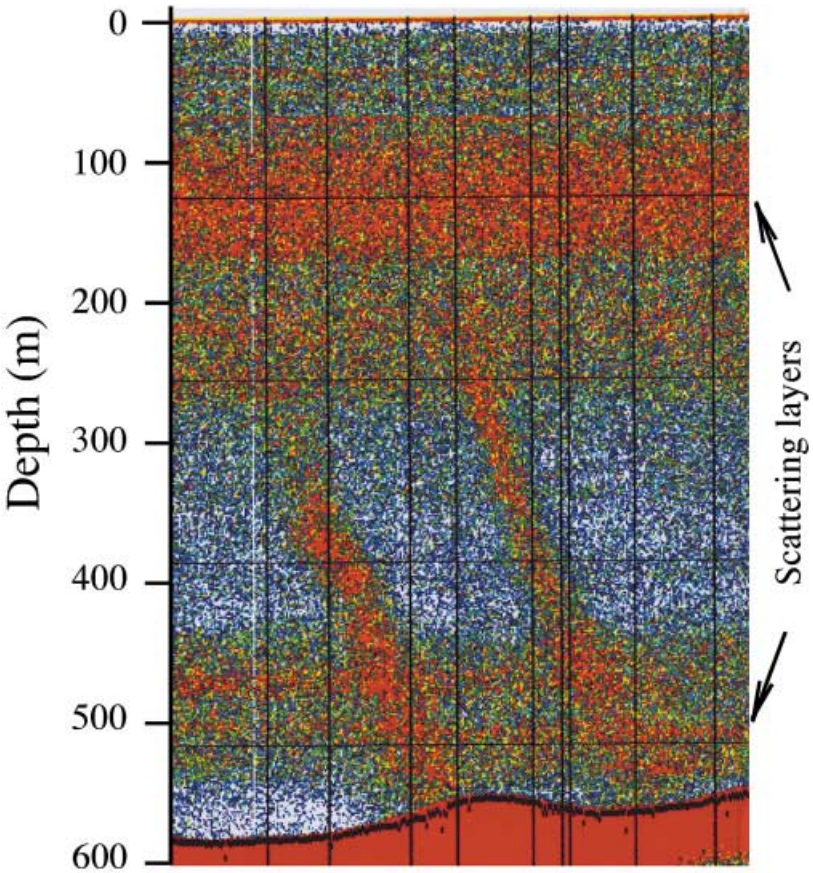

Fig. 3 Bush Hill, Gulf of Mexico (GC185), acoustic return (27°46.9′N, 91°30.4′W).

four or five relatively large (3–4 cm top diameter) bubbles (Hovland and Judd, 1988). The narrow size range is consistent with the data presented in Fig. 4, particularly for continuous streams.

In the extremely active SBC seeps, strong SBC upwelling flows of 30–100 cm s^{-1} were observed at the surface (Leifer *et al.*, 2000). For the GOM seeps, upwelling flows 1–15 cm s^{-1} were observed for three seeps at the seabed (Leifer and MacDonald, unpublished results). No observations to either confirm or deny the existence of upwelling flows for the North Sea seeps exist or were obtained.

Dissolved gas observations

Due to its extreme activity and shallowness, very high oceanic CH_4 levels, significantly above oceanic background levels, are observed in the SBC (Clark *et al.*, 2000). However, CH_4 in the water in the bubble plumes was significantly greater, slightly supersaturated with respect to the bubbles – i.e. CH_4 levels were millimolar (Leifer *et al.*, 2000). This is significant, since it is CH_4 in the plume rather than in the far field water that affects the bubble gas loss rate (discussed below). However, capturing plume water free of all bubbles is challenging.

Water is primarily transported into the North Sea site area from the North Atlantic by the Fair Isle Current and has low (2.5–3.5 nmol L^{-1}) CH_4 concentrations (Rehder *et al.*, 1994). River input is important in portions of the North Sea and contains significantly greater CH_4 (i.e. 100 nmol L^{-1} for the Rhine). However, based on the relationship between salinity and CH_4 in the North Sea for water entering from the Elbe River, the observed salinity (see Fig. 6) was consistent with background N. Atlantic CH_4 levels (Rehder *et al.*, 1994). One potential input near the site was a blow-out in November 1990 at 57°55′19.8′N, 1°37′56.9′E, ~ 30 km SE from the *Scanner* pockmark, that produced surface CH_4 levels in 1994 of 1450 nmol L^{-1}. Output from a dispersion model in Rehder *et al.* (1994) for the location of the *Scanner* pockmark estimated a decrease by a factor of ~ 100, i.e. potential blowout contribution to the study area was comparable to background levels.

The vertical CH_4 concentration profiles were determined for the North Sea site by water bottle casts above actively seeping pockmarks and in the field in general. Locations are shown in Fig. 1. The data has been segregated into profiles above pockmarks (Fig. 5A) and in the seep field (Fig. 5B). Average profiles for these two categories are shown in Fig. 5(C). Each profile was linearly interpolated to 1 m, and then averaged at each depth for profiles with available data. Three features are common to these profiles, a peak at 100–125 m depth, a deeper peak, and a gradual decrease from the shallower peak towards the surface. The deeper peak likely resulted from sediment disturbance during water bottle casts. The peak at 110 m is more pronounced for plumes than that for the field, but not significantly, namely the minimum at 130 m, or the decrease from 90 m towards the surface. The presence and consistent depth of this peak, both over pockmarks and away from pockmarks in several directions in the seep field area, strongly suggests that CH_4 was trapped in a layer. A least-squares, linear-regression analysis of the CH_4 decrease with depth from 100 m to the thermocline is shown in Fig. 5(C). Slopes were 0.35 and 0.81 nmol L^{-1} m^{-1}, with correlations of 69% and 83%, for the plume and field profiles, respectively.

During a May 1994 cruise, Rehder *et al.* (1994) observed a midwater column peak (~ 60 m depth) also below the thermocline at 57°43′N, 1.5°E, ~ 20 km from the blowout and ~ 70 km from the *Scanner* pockmark. During a North Sea transect at 58°N, a midwater peak was only observed at this site, while other sites just showed a peak below the thermocline.

Frequently, a CH_4 peak is observed at the thermocline (e.g. Fig. 5

© 2002 Blackwell Science Ltd

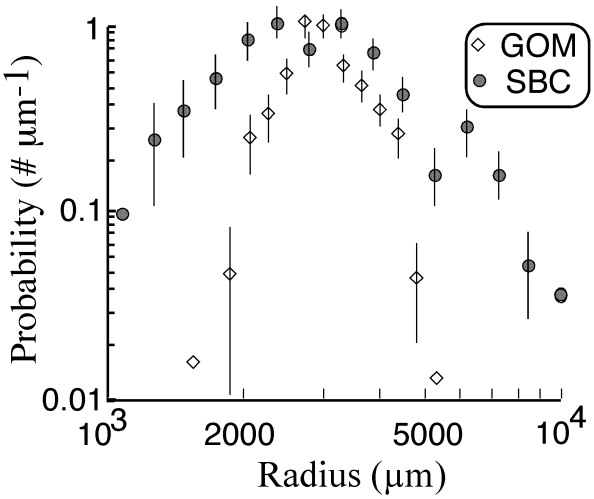

Fig. 4 Normalized bubble probability distributions (to peak probability = 1) for non-pulsing seep in the Gulf of Mexico (GOM) and combined pulsing and non-pulsing seep in the Santa Barbara Channel (SBC). Data key on figure.

No. 14); however, the thermal profile (Fig. 6) showed a very shallow thermocline. The *Challenger* pockmark (Nos. 6, 14) was the most active in terms of seepage and showed evidence of both the highest seepage and the highest CH_4 concentrations in near surface water.

Bubble gas exchange theory

Seep bubbles are often observed escaping from the seabed as a stream of nearly pure CH_4 bubbles (Hovland and Judd, 1988) with trace alkanes and atmospheric gases. The bubble CH_4 is highly supersaturated with respect to the bulk ocean and rapidly outflows from the bubble, causing bubble dissolution. The mass flux (F_M) for any gas from a bubble is described by (Leifer and Patro, 2002)

$$F_M = (\partial n/\partial t) = Ak_{\mathrm{B}}\Delta C = 4\pi r^2 k_{\mathrm{B}}(r, \mathbf{D}, T)(C - P_B/H(T)) \quad (1)$$

where n is the number of moles in the bubble, t is time, C is the aqueous concentration, ΔC is the concentration difference between the gas and liquid phases, r is the equivalent spherical radius, and A is the bubble surface area. The individual gas transfer rate (k_{B}) is strongly dependent upon r and the gas diffusivity (**D**). The bubble pressure (P_{B}) is primarily a function of the hydrostatic pressure (P_H) and H is the Henry's Law constant that describes the equilibrium between the gas concentration and the partial pressure. Both H and **D** are temperature (T) dependent.

A schematic of bubble gas exchange is shown in Fig. 7. As CH_4 outflows the bubble, the driving force, ΔC, decreases and thus F_M also decreases. While the CH_4 outflows the bubble, dissolved air inflows, slowing the rate

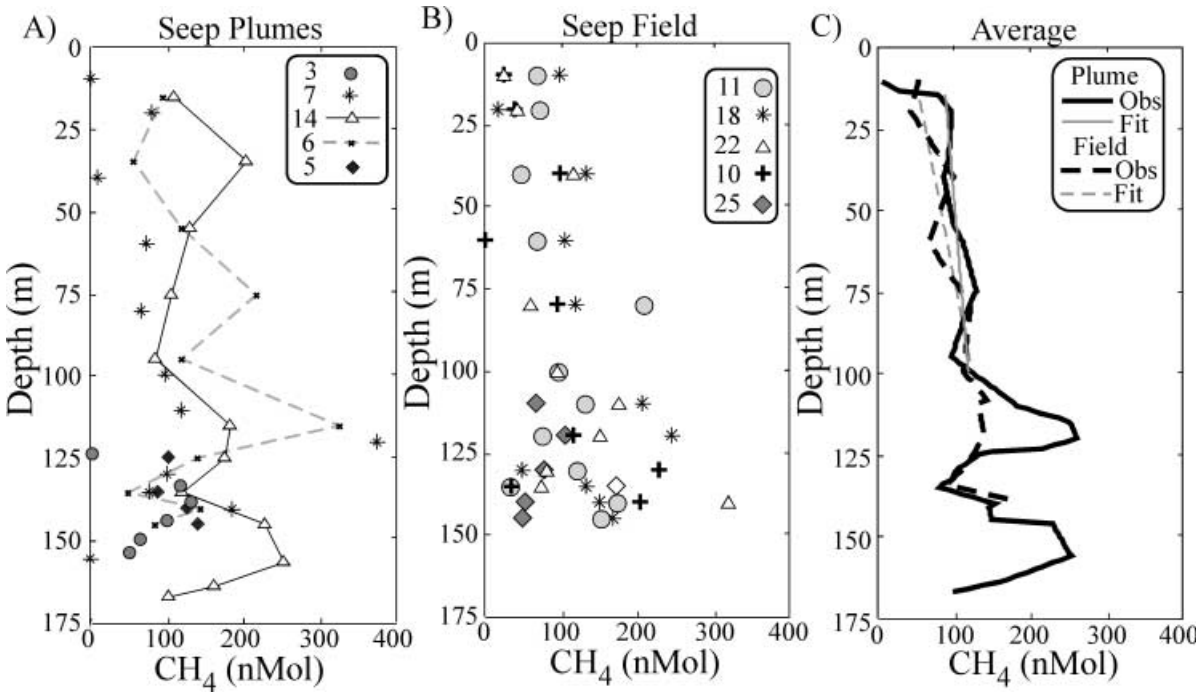

Fig. 5 CH_4 concentration profiles compiled from individual water bottle casts at locations over active pockmarks and distant from the seep field in the North Sea. For sample locations, see Fig. 1 and Table 1. (Data from Dando, 1991.)

 © 2002 Blackwell Science Ltd

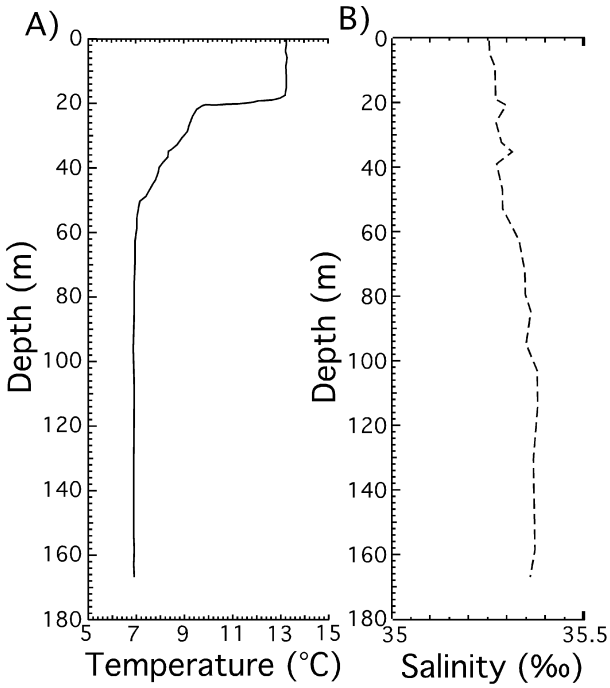

Fig. 6 Profile of temperature (A) and salinity (B) from a CTD cast at *Challenger* pockmark (Site 14). (Data from Dando, 1991.)

of bubble dissolution. Initially, air inflow has negligible effect on r (Fig. 7A), but as the bubble loses more CH_4 its air content becomes increasingly significant (Fig. 7B). In addition, the bubble grows due to the decrease in P_H as it rises (see Fig. 7B where the air inflow = CH_4 outflow). Complications arise if the bubble is in an upwelling flow, since $\partial P_H/\partial t$ is greater. Additionally, if the cumulative gas outflow from the plume bubbles increases C in the plume fluid, F_M decreases. The balance between these three processes determines whether or not a bubble dissolves. As a result, a bubble's fate depends, among other factors, upon its release radius (r_0), seabed depth (z_0), vertical velocity (V_Z), the rate $\partial P_H/\partial t$, and the aqueous CH_4 concentration (C).

Bubbles rise at their stagnant rise velocity (V_B) relative to the surrounding fluid, and also create upwelling flows. The upwelling flow, V_{up}, decreases the time for bubbles to reach the surface, as well as increasing $\partial P_H/\partial t$. For most seep bubbles, V_B is 20–30 cm s^{-1} and thus V_{up} can be significant, delaying bubble dissolution until shallower depths. Since the driving force behind V_{up} is the rising bubbles, bubble dissolution decreases V_{up}. This leads to our central hypothesis: if all plume bubbles dissolve, the upwelling flow will (after some distance) cease, causing both dissolved gases in the plume fluid and any particles or oil transported by the bubbles to be deposited at a subsurface depth.

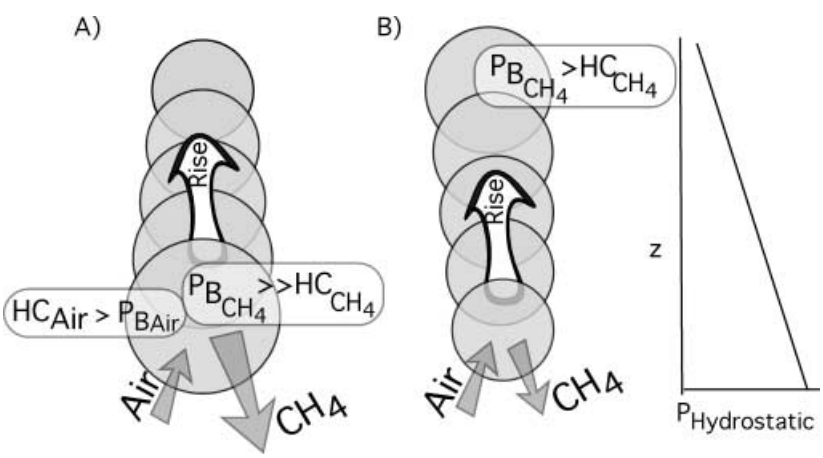

Fig. 7 Schematic of seep bubble gas exchange. In (A) CH_4 outflow is much greater than air inflow, and the bubble size decreases; in (B) air inflow matches CH_4 outflow, but the bubble size increases because the pressure (P_H) decreases as the bubble rises.

Numerical bubble model

Bubble dissolution for North Sea hydrocarbon seepage was investigated with a numerical bubble model (described in detail in Leifer and Patro, 2002). A model flowchart is shown in Fig. 8. Initially, physical, fluid dynamical, plume and chemical parameters are loaded. Next, the seabed bubble flux distribution, $\phi(r)$, is calculated from the product of the observed $V_B(r)$ and the size probability distribution – i.e. Fig. 4. Where feasible, look-up tables are calculated for calculation speed, including parameterizations for k_B and V_B. Bubbles in each size class are simulated including an imposed upwelling flow, V_{up}. The model solves the coupled differential equations describing the change in n, r, P_B and z as a bubble rises, exchanges gases, and changes in size due to gas exchange and decreasing P_H. Then the output for each r is interpolated to a smooth depth grid. The mass flux for the plume at each depth can be calculated from the bubble mass flux integrated over the bubble flux at each depth. **D** and H were for 6.9 °C (from Wanninkhof, 1992).

For this study the model simulated bubbles spanning $100 < r < 10^4$ μm with varying surfactant contamination, where small bubbles are dirty, and large bubbles are clean (Patro *et al.*, 2001) with a transition at $r = 500$ μm, from a release depth of 172 m (*Challenger* pockmark). V_{up} was constant throughout the water column. In reality, V_{up} decreases as the plume disperses and bubbles dissolve, disappearing if all bubbles dissolve unless the plume fluid is more

© 2002 Blackwell Science Ltd

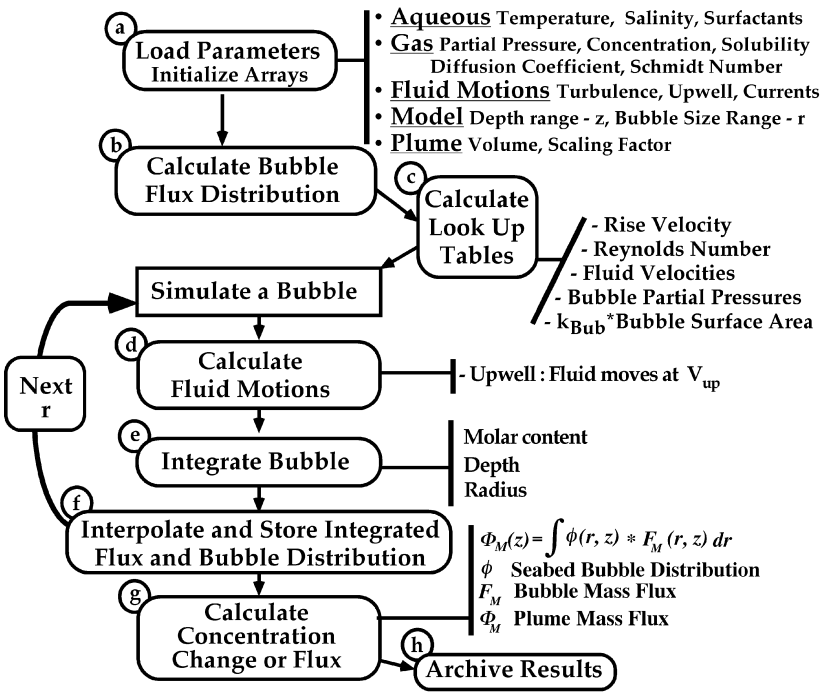

Fig. 8 Flowchart of numerical bubble model.

buoyant than the surrounding ocean (i.e. T increases with depth). Gas parameters are shown in Table 1. Since bubble air content and aqueous values were unavailable, air in the bubbles was assumed trace, using values from SBC seabed seep composition – Leifer *et al.* (2000). The remaining bubble content was simulated as pure CH_4. Average T and CH_4 values for the lower 100 m (from Figs 5 and 6) were used. Over z of interest for this study ($172 < z < 100$ m), sensitivity studies showed that the observed z variations in T and CH_4, had negligible effect on the model calculations, and therefore using water-column averaged values was appropriate.

Model results

The calculated ratio of the final (i.e. surface) to initial r is shown in Fig. 9(A), while for dissolving bubbles, the dissolution depths are shown in Fig. 9(B), for upwelling flows, V_{up}, of 0, 5 and 10 cm s^{-1}. For all cases the smallest bubbles dissolved close to the bottom. For $V_{up} = 0$ cm s^{-1}, bubbles smaller than 3400 μm dissolved subsurface; while with increasing V_{up}, smaller bubbles survived and larger bubbles grew more. For $V_{up} =$ 10 cm s^{-1}, only $r < 2500$-μm bubbles reached the surface. For this range of V_{up}, bubbles ~ 2700 μm dissolved from 110 m ($V_{up} = 0$) to 60 m ($V_{up} = 10$). Clearly, bubble size and V_{up} are critical.

Discussion and conclusions

Our hypothesis is that the bubbles outflow methane into the surrounding upwelling fluid that ceased rising near the depth where the bubbles dissolved, forming the observed layer. The model results show that the predicted dissolution depth for *Challenger* was slightly shallower than the observed methane peak, particularly if $V_{up} > 0$. The $V_{up} = 0$ simulation is an unrealistic limiting case, since in the absence of an upwelling flow, it is very difficult to produce a CH_4 peak. This is because the bubble gas flux is greatest initially, i.e. near the seabed (when ΔC is greatest), and thus the CH_4 peak would be near the seabed – a feature more strongly observed over the pockmarks.

The crucial question for interpreting the model output is: For what z does $V_{up} = 0$? This is critical, since it is at this z that the plume stops rising and is 'pulled' in the downcurrent direction, forming a deposition layer. Unfortunately, theoretical understanding of upward rising oceanic bubble plumes is virtually non-existent, with few measurements available, particularly throughout the water column. Therefore, we approach this question descriptively.

The more developed is a bubble wake, the more efficiently the bubble transfers momentum to the rising plume. The flow around $r < 300$-μm bubbles is close to laminar, while oscillating bubbles ($r > 900$ μm) have well-developed wakes (Clift *et al.*, 1978). Thus for $r \sim 300$ μm, the driving force for V_{up} is likely to disappear. However, due to inertia, the plume should rise somewhat higher. Bubbles will dissolve to 300 μm below the dissolution depths shown in Fig. 9. For example, for $V_{up} = 0$ and 5 cm s^{-1}, 2000-μm bubbles dissolved to 300 μm, 5 m and 10 m below their respective dissolution depths. For higher V_{up} the dissolving bubbles were advected further upwards. Thus the model is consistent with V_{up} disappearing and forming a layer ~ 10 m below the bubble dissolution depth.

If the emitted size distribution of bubbles is narrow, all bubbles will dissolve at about the same depth, i.e. in a thin layer. Thus, any substances carried by the bubbles, e.g. sediment, mineral particles, bacteria, etc., in addition to methane in the rising upwelling flow, will be deposited in a subsurface layer. For oily bubbles this implies a subsurface oil layer. Bubbles are known to efficiently accumulate and transport surface active bacteria, particles and surfactants (Blanchard,

Table 1 Gas parameters for simulations. C_S is the saturation pressure

	CH_4	O_2	N_2
P (Atm)	17	0.0241	0.136
C (mol l^{-1})	2.00×10^{-7}	9.76×10^{-5}	1.37×10^{-4}
H (Atm mol^{-1} L^{-1})	609	1430	695
C_S (mol L^{-1})	2.79×10^{-2}	1.69×10^{-5}	1.96×10^{-4}
D (cm^2 s^{-1})	1.0×10^{-5}	1.12×10^{-5}	9.9×10^{-6}

 © 2002 Blackwell Science Ltd

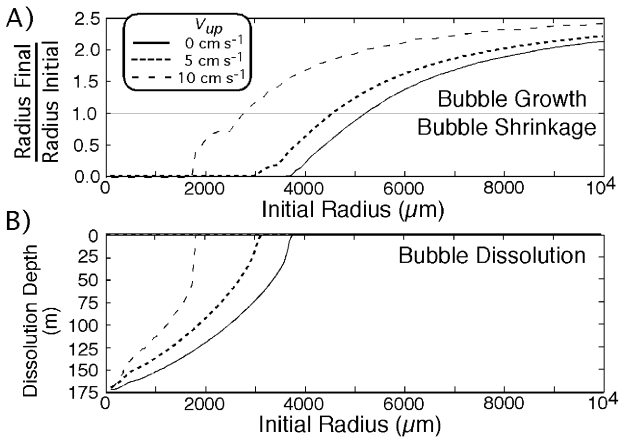

Fig. 9 Calculated final to initial radius (A) and dissolution depths (B) for different size bubbles for three upwelling flows. Data key on figure.

1989), and are important to sustaining the enhanced level of such in the sea surface microlayer (Grammatika and Zimmerman, 2001). These materials may arise from the seep, or be collected (sparged) from oceanic water and be deposited in a bubble deposition layer.

Particle deposition in such a layer may produce a layer enriched in nutrients that marine organisms may find attractive. During several surveys of this area, gas plumes have been observed rising from the *Scanner*, *Scotia* and *Challenger* pockmarks, but never from elsewhere in the area. The gas is rising from beneath the surficial Quaternary sediments (Judd *et al.*, 1994); apparently, these pockmarks are sited over the only active gas migration pathways. The hyperbolic targets shown in Fig. 2 indicate the presence of gas bubbles, which may or may not be located inside marine organisms. Support to the marine organism interpretation is the widespread distribution in a layer at 120–140 m, and their character. Rising bubble plumes leave a trail (i.e. Fig. 3), while bubble pulses are unlikely to be found in a layer, particularly since bubble pulses (including pulses observed at this site) include large bubbles that can reach the surface (Fig. 9). Further evidence for a biological explanation was recorded on submarine video and in submarine operator comments regarding significant numbers of jellyfish at 120–140 m depth. In addition, during several different cruises, many tentacles of the same species of jellyfish (*Cyanea lamarckii*) were retrieved from the same depth attached to coring cable. Thus jellyfish and/or other organisms may explain the targets.

While possibly coincidental, this research demonstrates a potential mechanism to explain the co-location of these hyperbolic targets and the midwater-column methane layer evidenced in Fig. 5. Clearly this evidence is insufficient to prove a relationship between bubble dissolution and enhanced biological activity. However, we regard this hypothesis of sufficient probability to merit further detailed investigation of the role of seep bubble plumes in nutrient cycling within the water column. Such studies are needed to investigate the nature and fates of seep bubbles, the variability of CH_4 concentrations within the water column, and distribution and density of organisms within the water column.

The correlation for the linear fit of the CH_4 profile to depths above the 115-m peak was high, indicating that the profile is primarily explained by a deep CH_4 source (the layer) and is consistent with loss due to vertical mixing and an upwards flux. The profile is consistent with an upwards CH_4 flux to the thermocline. The CH_4 slope within the plume is less steep than outside, indicating either a greater upwards flux or additional input from larger bubbles. However, model predictions show that a bubble source flux decreases exponentially with height above the seabed (Leifer and Patro, 2002), while here the profile decreased linearly. Thus one explanation is that the higher CH_4 concentration at shallower depths in the plume is due to the effect of the observed very-large-diameter bubbles on vertical mixing rates. Finally, the presence of a vertical flux to the base of the mixed layer over an area covering tens of square kilometres suggests a non-negligible fraction of the seep methane may escape into the atmosphere.

In this paper we have demonstrated a conceptual model showing how a rising bubbly flow from a seep can form a deposition layer of methane and nutrients when the bubbles dissolve. This also has implications for understanding the fate of oil in the ocean from both natural hydrocarbon seeps or oil/gas leaks related to petroleum exploitation. When present, oil will be deposited in the same subsurface layer as the methane and other particles. Predictions were consistent with estimated bubble sizes and constrain the upwelling flow magnitude. The dissolution depth was shown to depend upon bubble size and upwelling flow strength. This depth may depend upon other factors such as bubble cleanliness, methane concentration in the plume water, and stratification (where changes in T etc. may significantly alter the bubble dissolution depth). Therefore, we hypothesize that the influence of seeps on the food chain may not be confined to the benthic community in the immediate seep vicinity.

Acknowledgments

The support of the Mineral Management Service and the University of California Energy Institute are gratefully acknowledged. Data for the North Sea were acquired during the Challenger 82 cruise of *RRV Challenger* (Chief Scientist Paul Dando), and during a survey on *Kommander Jack*, funded by the UK government's Department of Trade and Industry as part of a Strategic Environmental Assessment of the mature oil and gas provinces of the North Sea being carried out in 2001 and managed by Geotek Ltd. We are also grateful for the facilities and help for the crew of the *Johnson Sea Link* during the cruise to Gulf of Mexico and the support of Ian MacDonald.

© 2002 Blackwell Science Ltd

References

Blanchard, D.C., 1989. The size and height to which jet drops are ejected from bursting bubbles in sea water. *J. Geophys. Res.*, **94**, 10,999–11,002.

Brooks, J.M., Kennicutt, II M.C., Fay, R.R., McDonald, I.J. and Sassen, R., 1984. Thermogenic gas hydrates in the Gulf of Mexico. *Science*, **223**, 696–698.

Chen, R.C., Reese, J. and Fan, L.-S., 1994. Flow structure in a three-dimensional bubble column and three-phase fluidized bed. *Aiche J.*, **40**, 1093–1104.

Clark, J.F., Washburn, L., Hornafius, J.S. and Luyendyk, B.P., 2000. Dissolved hydrocarbon flux from natural marine seeps to the Southern California Bight. *J. Geophys. Res.*, **105**, 11,509–11,511,522.

Clift, R., Grace, J.R. and Weber, M.E., 1978. *Bubble, Drops and Particles*. Academic Press, New York.

Dando, P.R., 1991. *RRS 'Challenger' Cruise 82 Report, Marine*. Biological Association of the United Kingdom.

Dando, P.R., 2001. *A Review of Pockmarks in the UK Part of the North Sea, with Particular Respect to Their Biology*. Technical Report TR_001, Strategic Environmental Assessment – SEA2, Department of Trade and Industry, London.

Dando, P.R., Austen, M.C., Burke, R.A., Jr Kendall, M.A., Kennicutt, M.C., I.I.Judd, A.G., Moore, D.C., O'Hara, S.C.M., Schmaljohann, R. and Southward, A.J., 1991. Ecology of a North Sea pockmark with an active methane seep. *Mar. Ecol. Prog. Ser.*, **70**, 49–63.

Dando, P.R. and Hovland, M., 1992. Environmental effects of submarine seeping natural gas. *Cont. Shelf Res.*, **12**, 1197–1208.

Fleischer, P., Orsi, T.H., Richardson, M.D. and Anderson, A.L., 2001. Distribution of free gas in marine sediments: a global overview. *Geo-Mar. Lett.*, **21**, 103–122.

Grammatika, M. and Zimmerman, W.B., 2001. Microhydrodynamics of flotation processes in the sea surface layer. *Dyn. Atmos. Oceans*, **34**, 327–348.

Guinasso, N.L. Jr and Schink, D.E., 1973. *A simple physico-chemical acoustic model of methane bubbles rising in the sea*. Texas A & M University, Houston, unpublished report.

Hornafius, J.S., Quigley, D.C. and Luyendyk, B.P., 1999. The world's most spectacular marine hydrocarbon seeps (Coal Oil Point, Santa Barbara Channel, California): Quantification of emissions. *J. Geophys. Res.*, **104**, 20703–20711.

Hovland, M. and Judd, A.G., 1988. *Seabed Pockmarks and Seepages*. Graham and Trotman, London, pp. 293.

Hovland, M. and Sommerville, J.H., 1985. Characteristics of two natural gas seepages in the North Sea. *Mar. Petrol. Geol.*, **2**, 319–326.

Hovland, M. and Thomsen, E., 1989. Hydrocarbon-based communities in the North Sea? *Sarsia*, **74**, 29–42.

Jakobsen, H.A., Sannaes, B.H., Grevskott, S. and Svendsen, H.F., 1997. Modeling of vertical bubble-driven flows. *Ind. Eng. Chem. Res.*, **36**, 4052–4074.

Johansen, Ø., 2000. DeepBlow – A Lagrangian plume model for deep water blowouts. *Spill Sci. Techn Bull.*, **6**, 103–111.

Judd, A.G., 2000. Geological sources of methane. In: *Atmospheric Methane: It's Role in the Global Environment* (M.A.K. Khalil, ed.), pp. 280–303. Springer Verlag, New York.

Judd, A.G., Hovland, M., Dimitrov, L.I., García Gil, S. & Jukes, V., 2002. The geological methane budget at continental margins and its influence on climate change. *Geofluids*, **2**, 109–126.

Judd, A.G., Davies, G., Wilson, J., Holmes, R., Baron, G. and Bryden, I., 1997. Contributions to atmospheric methane by natural seepages on the UK continental shelf. *Mar. Geol.*, **137**, 427–455.

Judd, A.G. and Hovland, M., 1989. The role of chemosynthesis in supporting fish stocks in the North Sea. *J. Fish Biol. A*, **35**, 329–330.

Judd, A.G., Long, D. and Sankey, M., 1994. Pockmark formation and activity, U K block 15/25, North Sea. *Bull. Geol. Soc. Denmark*, **41**, 34–49.

Juhl, A.R. & Targon. G.L., 1993. Biology of an active methane seep on the Oregon continental shelf. *Mar. Ecol. Prog. Series*, **102**, 287–294.

Keeling, R.F., 1993. On the role of large bubbles in air-sea gas exchange and supersaturation in the ocean. *J. Mar. Res.*, **51**, 237–271.

Kvenvolden, K.K., Reeburgh, W.S. and Lorenson, T.D., 2001. Naturally occurring methane seepage—Workshop report 2001. *EOS*, **82**, 457.

Leifer, I., Clark, J. and Chen, R., 2000. Modifications of the local environment by a natural marine hydrocarbon seep. *Geophys. Res. Lett.*, **27**, 3711–3714.

Leifer, I. and Patro, R., 2002. The bubble mechanism for transport of methane from the shallow sea bed to the surface: a review and sensitivity study. *Cont. Shelf Res.*, **22**, 2409–2428.

MacDonald, I.R., Guinasso, N.L., Jr Ackleson, S.G., Amos, J.F., Duckworth, R., Sassen, R. and Brooks, J.M., 1999. Natural oil slicks in the Gulf of Mexico visible from space. *J. Geophys. Res.*, **98** (C9), 16351–16364.

Monahan, E.C. and Spillane, M.C., 1984. The role of oceanic whitecaps in air-sea gas exchange. In: *Gas Transfer at Water Surface* (W. Brutsaert and G. H. Jirka., eds), pp. 495–503. D. Reidel Publications Co, Dordrecht.

Patro, R., Leifer, I. and Bowyer, P., 2001. Better bubble process modeling: Improved bubble hydrodynamic parameterization. In: *Gas Transfer at Water Surfaces* (M.A. Donelan, W.M. Drennan, E.S. Saltzman and R. Wanninkhof, eds). *AGU Monogr.*, **127**, 315–320.

Quigley, D.C., Hornafius, J.S., Luyendyk, B.P., Francis, R.D., Clark, J. and Washburn, L., 1999. Decrease in natural marine hydrocarbon seepage near Coal Oil Point, California, associated with offshore oil production. *Geology*, **27**, 1047–1050.

Rehder, G., Keir, R.S., Suess, E. and Pohlmann, T., 1994. The multiple sources and patterns of methane in North Sea waters. *Aquat. Geochem.*, **4**, 403–427.

Wanninkhof, R., 1992. Relationship between wind speed and gas exchange over the ocean. *J. Geophys. Res.*, **97** (C5), 7373–7382.

Zheng, L. and Yapa, P.D., 1998. Simulation of oil spills from underwater accidents II: Model verification. *J. Hydraulic Res.*, **36**, 117–134.

Received 23 October 2001; revised version accepted 4 July 2002

 © 2002 Blackwell Science Ltd